BATCH MODE MICROMANUFACTURING BASED ON MICRO ELECTRO-DISCHARGE MACHINING AND MICRO ULTRASONIC MACHINING FOR MICRO ELECTRO MECHANICAL SYSTEMS (MEMS)

Tao Li and Yogesh B. Gianchandani
Engineering Research Center for Wireless Integrated Microsystems
University of Michigan, Ann Arbor, MI, USA

ABSTRACT

Metal alloys have material properties that are very appealing for micro electro mechanical systems (MEMS), but present a challenge for process integration within a lithographic manufacturing sequence of the type used in the semiconductor industry. The batch-mode micro electro-discharge machining (μEDM) discussed here uses lithographically-fabricated electrode arrays with high density and high uniformity to achieve high-throughput and high-precision micromachining. It has been demonstrated for potential applications that range from micro-gears to smart stents. Similarly, batch-mode micro ultrasonic machining provides lithographic manufacturing compatibility to micromachining hard ceramics and other dielectric materials, such as glass-mica ceramic, lead zirconate titanate (PZT), single-crystal quartz, ruby, etc. In this process, batch-μEDM is used to define a cutting tool with desired pattern, typically in stainless steel. This has been demonstrated for the batch fabrication of piezoelectric transducers for smart biopsy tools and structurally complex microresonators.

I. INTRODUCTION

In the last several decades, the emergence and rapid development of micro electro mechanical systems (MEMS) have largely relied on established semiconductor manufacturing technologies for integrated circuits (IC). Micromachining processes for silicon have been extensively used for fabrication of MEMS sensors and actuators. The lithography-based batch manufacture of these devices has allowed high throughput and low cost, and monolithic integration with microelectronic circuits for increased functionality and performance. However, these machining processes generally favor silicon, some polymers and thin films of select metals and dielectrics. The means to add bulk materials are limited, particularly for metal alloys. Electroplating is typically restricted to gold, copper and nickel. Other additive processes such as micromolding of ceramics can have issues of volume shrinkage and non-uniform material properties, especially at the micro scale. In contrast, subtractive processes on bulk materials offer superior control of material properties and uniformity. Lack of diversity in bulk material choices for device structures has limited the functionality and performance of many MEMS devices, and often impedes the development of new and potential MEMS applications. Thus, lithography compatible micromachining technologies capable of handling broader range of bulk materials remain highly desirable.

One category of bulk materials of interest is high strength and refractory metals and alloys such as steel, titanium (Ti), and platinum-rhodium (Pt-Rh). Steel has played important roles in macro-scale applications, but has not been explored for use in MEMS. Ti is well recognized for its biocompatibility and has been used for packaging in implantable devices such as pacemakers, but in the MEMS field it has been primarily used in thin films. Pt-Rh has a proven history in chemically harsh environments but not for MEMS. These constraints can be addressed by batch-mode micro electro-discharge machining (μEDM) [1]. This is a lithography-based bulk-micromachining technology that can handle any conductive materials, including metals and alloys.

Another important category of bulk materials is ceramics, which in broad definition refer to any non-metallic and non-organic solid materials. Ceramics offer important properties such as high electrical and thermal insulation, high melting temperature, and high chemical stability. Piezoelectric ceramic materials, such as lead-zirconate-titanate (PZT), have been widely used in sensors and actuators. However, in the MEMS area PZT has mostly been used as deposited thin film, which compromises material properties. Although there are already subtractive technologies that can process ceramics for MEMS applications, there are limitations. For example, plasma etching methods, such as reactive ion etching (RIE), have limited etching rate and require different gas chemistry for different ceramics. Lithography-based pattern transfer to ceramics still remains a challenge. Ultrasonic machining (USM), which is a highly effective technology for any hard and brittle material, can be a promising candidate. At the micro scale, it has mostly been used in serial mode, limiting its throughput and capability to handle complex patterns. Batch-mode micro ultrasonic machining (μUSM) process provides the capability of lithographic pattern transfer on any hard and brittle materials including ceramics and glasses [2].

In the following sections, the details of batch mode μEDM and batch mode μUSM will be described and some of the applications to date will be presented.

Corresponding author: 1301 Beal Ave., Ann Arbor, MI, 48109, USA; Tel: 1-734-615-7983, Fax: 1-734-763-9324, Email: litz@umich.edu

II. BATCH MODE μEDM

The μEDM process can be used to machine 3D microstructures from any electrically conductive material, including steel, graphite [3], silicon [4], and magnetic materials such as permanent magnets [5]. When combined with lithography technology, μEDM can be used in batch mode, providing high spatial density, high uniformity, and much higher throughput compared with serial mode μEDM [1].

Overall Process Description

The μEDM process involves the sequential discharge of electrical pulses between a microscopic electrode and the workpiece while both are immersed in dielectric oil [6]. The pulse discharge timing is controlled by a simple RC circuit. The electrode is conventionally a cylindrical metal element that has a minimum demonstrated diameter of ≈5 μm. The electrodes can be individually shaped by using a μEDM technique known as wire electro-discharge grinding (WEDG) [7]. The use of a single electrode that is scanned or scrolled across the sample surface for machining is referred to as the serial mode μEDM. A typical machine for this purpose was originally developed by Panasonic, Inc. Enhanced models are now available from SmalTec, LLC. In order to achieve micron-scale precision, the apparatus uses an extremely small amount of discharge energy (10^{-7} J level) and submicron accuracy in spindle rotation, feeding, and positioning. Submicron tolerance and fine surface finish of 0.1 μm R_{max} roughness have been demonstrated [6].

Although it has been commercially used for applications such as ink-jet nozzle fabrication, the serial μEDM method is limited in throughput. This is especially true for complex patterns such as gears, which require contour scanning along the edge of the patterns. Batch mode μEDM, which uses lithographically-fabricated electrode arrays, can overcome this limitation [1,8]. The concept is shown in Fig. 1. By using precisely located high-aspect-ratio electrode arrays fabricated by lithography and electroplating processes, the batch mode μEDM process can provide not only high throughput but also high spatial density and uniformity over the whole machining area. Electroplated copper is used as the electrode material because it has high melting point and high thermal conductivity for minimized wear of the electrodes. The LIGA process, which is the German acronym for lithography, electroplating, and molding, can be used to form exceptionally high-aspect-ratio molds for electroplating by deep X-ray lithography [9]. During machining, the whole electrode array (cathode) is fed into the workpiece (anode); discharges are fired and the whole pattern is transferred onto the workpiece [1].

The array of electroplated Cu electrodes fabricated on a carrier substrate provides spatial multiplicity in the electrical discharges. However, if the electrodes are all connected in parallel to the same pulse generation circuit, only one tends to fire at any given moment. By separating arrayed electrodes into segments that are independently
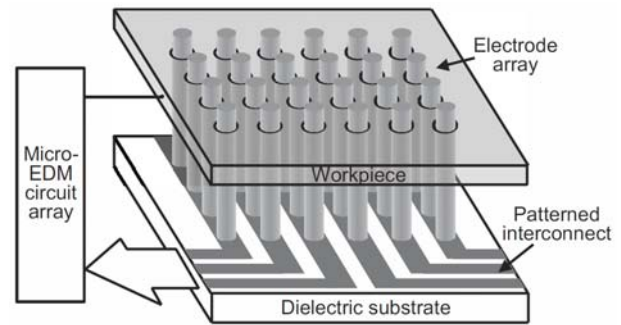

Fig. 1: Concept of batch mode μEDM with single pulse generating circuit [1].

controlled, it is possible to achieve both spatial and temporal multiplicity, providing machining throughput that is orders of magnitude higher than is possible by a serial approach. This is referred to as parallel discharge. It can be facilitated, in part, by utilizing the parasitic on-chip capacitance between the electrodes and the Si substrate as a design component within the pulse timing circuit. Not only does this provide a compact solution, but the resulting elimination of the parasitic nature of the capacitance provides superior control over the size and timing of the pulses, improving the precision of the machining and reducing crosstalk between electrodes. Using this mode of operation, a throughput >100× higher than that of serial μEDM with a single electrode has been demonstrated [1].

With the introduction of the batch mode concept, the shaping capability, feature density, throughput, and uniformity of μEDM technology has been greatly improved. Although it is not suitable for machining dielectric materials, the capability of EDM to handle hard metals such as tool steel and WC/Co makes it an attractive technique for preparing cutting tools which can be used to mechanically machine dielectrics. This is discussed in Section III.

Tackling the Debris Buildup Issue

During the μEDM process, debris accumulation between the electrode and workpiece can lead to spurious discharges that damage the workpiece surface and cause excessive tool wear. In batch mode μEDM, this can become even more serious due to the large area and small separation of the tool from the workpiece, and can cause uncontrolled arcing and stall the machining indefinitely. A parametric study of the batch mode μEDM of high density features in stainless steel confirmed that, when the tool feature density is increased, the effect of debris accumulation begins to dominate and eventually degrades both tool and workpiece [10]. Two independent techniques for mitigating this debris buildup have been proposed [10]. The first is a passivation coating which suppresses spurious discharges triggered from the sidewalls of the machining tool. By this method, the mean tool wear rate decreases from a typical of about 34% to 1.7% and machining non-uniformity reduces from 4.9 μm to 1.1 μm across the workpiece. The second technique involves a two-step machining process that enhances the hydrodynamic removal of machining debris compared to standard methods. By

first µEDM'ing narrow through-holes in the workpieces at selected locations across the machining area, a path is created for the debris to escape when the overlaid, final pattern is machined. This improves surface and edge finish of the machined features, machining time and tool wear.

Wireless Process Monitoring

Traditional methods of monitoring EDM machining quality rely on electrical characteristics at the discharge supply terminals. Inherent wireless signals generated with each discharge in µEDM can be used for direct observation of discharge quality. This wireless method is less affected by electrical parasitics in the supply loop and by spatial averaging. This approach has been shown to help address two significant challenges in µEDM: sensing a material transition within a workpiece, and sensing excessive debris accumulation [11]. The depth location of a metal-metal interface can be distinguished in the wireless signal. This is useful for determining the stop depth in certain processes. For example, in machining through samples of stainless steel into an electroplated copper backing layer, the metal transition is identified by a 10-dBm change in wireless-signal strength for a 300-350 MHz band and a 5 dBm average change across a full 1 GHz bandwidth. This can be applied to separate stacked metals as well. As debris accumulate in the discharge gaps, shifts in the wireless spectra can also indicate spurious discharges that could damage the workpiece and tool. For example, when copper micromachining becomes debris dominated, an 800-850 MHz band drops 4 dBm in signal strength, with a 2.2 dBm average drop across a full 1 GHz bandwidth.

III. BATCH MODE µUSM

Conventional USM has been widely accepted as an effective machining process for hard and brittle materials like ceramics, glass, etc. These materials are brittle and are more easily fractured than plastically deformed. Hence, USM produces little or no damage or high-stress deformation at or below the surface. Moreover, it causes no thermal or chemical alterations in the sub-surface characteristics of the machined material [12]. However, USM at the micro level has been mostly utilized in a serial approach with a single rotating tool, limiting both throughput and structural shapes [13,14]. The batch mode µUSM approach facilitates parallel transfer of complex lithographic patterns and provides relatively high resolution and throughput, while retaining the favored characteristics of conventional USM [2].

Overall Process Description

A candidate process flow is shown in Fig. 2. First, hard-metal (*e.g.* steel) microtools with desired patterns are made by micro electro-discharge machining (µEDM). This can be performed in batch mode for compatibility with lithographic methods (LEEDUS) [1], or serial mode for rapid prototyping of simple patterns (SEDUS). Multi-level structures can also be defined in the microtools [15]. For batch mode operation, electroplated copper structures can
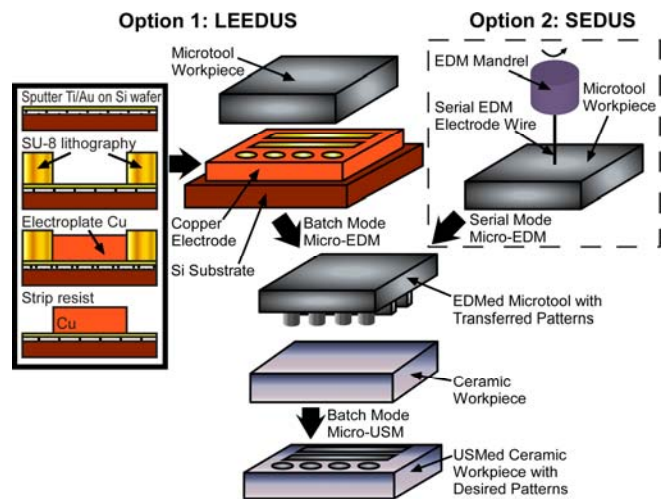

Fig. 2: *LEEDUS process utilizes lithography, electroplating, and batch mode µEDM to fabricate a microtool with a pattern which is defined by a mask, and then uses batch mode µUSM to transfer the pattern onto ceramic or other brittle materials. Non-lithographic rapid-prototyping can also be performed for simple patterns using option 2 (SEDUS) [2].*

be formed using SU8 or LIGA molds with lithographically-defined patterns. These copper structures are then used as an electrode for batch µEDM to transfer the patterns onto hard metal substrates for microtools. Non-lithographic rapid-prototyping can be performed for simple patterns by the original serial function of a Panasonic/SmalTec µEDM machine. A program on a computer controls the "writing" movement of the rotating µEDM electrode on the microtool substrate as well as different cutting depths for multi-level structures.

The microtool is then mounted on a custom-built setup for batch mode µUSM, and the patterns on the microtools are transferred onto a ceramic workpiece. Abrasive slurry, which consists of water and fine abrasive powders, is supplied between the tip of the microtool and the workpiece. The vibrating tip of the microtool is fed into the workpiece. The ultrasonic motion of the microtool imparts velocity to the abrasive particles on its downward stroke. These particles, in turn, are responsible for the erosion of the workpiece, thus creating the desired cavities in the shape of the microtool.

Both dynamic force detection and acoustic emission (AE) detection have been used to monitor the µUSM process [2,15]. The dynamic force detection approach uses wideband piezoelectric sensors and can be used to directly measure the machining load. In contrast, the AE sensor detects the higher-frequency transient elastic waves generated by microchipping that occurs in the workpiece during µUSM, while filtering out the main frequency component of vibration from the ultrasound generator. This provides an effective measure of the actual machining.

Batch-mode µUSM has been successfully applied to Macor® glass ceramic [2], PZTs [2,], single-crystal quartz [15], Zerodur® [15], ruby and glasses [16], etc. Feature sizes <25 µm have been batch fabricated. Cutting
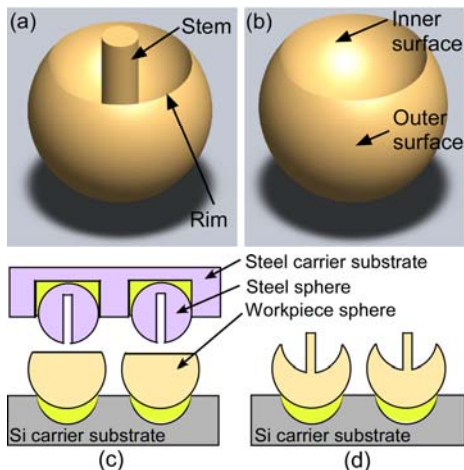
3

Fig. 3: Schematic of the (a) mushroom and (b) concave shaped spherical structures fabricated using the 3D-SOULE process. (c)-(d): Process illustration for the mushroom structure [16].

depths >350 µm and cutting rates >24 µm/min. have been demonstrated.

3D Micromachining of Spherical Geometries

Three dimensional (3D) microstructures in hemispheric, "wine glass" and mushroom shapes (Fig. 3a-b) made from high quality factor (Q) materials, *e.g.* fused quartz, are attractive for some types of inertial sensors, such as rate integrating gyroscopes [17,18]. However, these materials cannot be easily micromachined into 3D geometries with either conventional lithography-based technologies or melting/reflow, and are difficult to integrate with silicon or other substrates. A lithography-compatible method for integrating and micromachining concave and mushroom-shaped spherical structures made from these materials has been developed. The 3D-SOULE process [16] is a 3D-capable and self-aligned process combining batch-mode µUSM, lapping, and µEDM. The tool is prepared by embedding separately-manufactured high-grade steel spheres onto a steel substrate with µEDM'ed cavities, to form an array of spherical features for batch machining (Fig. 3c). Holes can also be made into the steel spheres to form the stems of the target mushroom structures. The tool is then used in batch-mode µUSM of a silicon carrier substrate
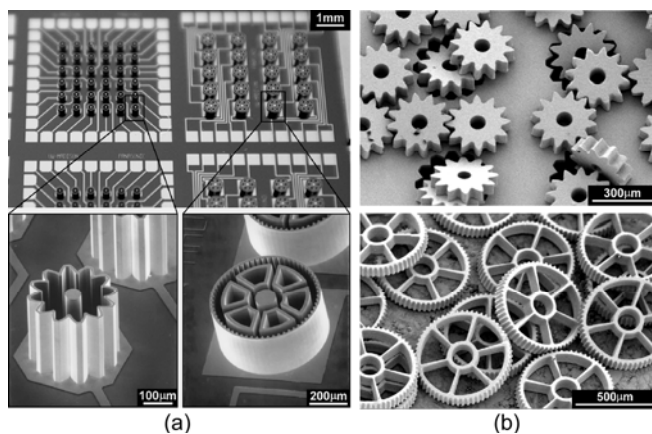

Fig. 4: (a) Monolithic copper electrode arrays with patterned interconnect. (b) WC-Co super hard alloy gears batch-cut from a 70-µm thick workpiece using electrode arrays shown in (a) [1].

to make an array of shallow spherical cavities. Separately-manufactured fused quartz spheres are then embedded into these cavities, allowing self-alignment between the tool steel spheres and the target fused quartz spheres. Finally, a second batch-mode µUSM step is done with the same tool to form the mushroom (Fig. 3d) or concave (when no holes are made into the tool spheres) geometries. Since µUSM does not involve any chemical or high temperature steps, it is possible to create stress-free structures in a wide variety of ceramics, glasses and other brittle materials.

IV. APPLICATIONS

The µEDM and µUSM processes have been applied to the implementation of a variety of MEMS sensors and actuators. Several examples of the demonstrated applications are presented in this section.

Batch Microfabricated Gears

Using the parallel discharge approach in batch mode µEDM, a monolithic partitioned electrode array with multiple pulse generating circuits was fabricated by a two-mask sacrificial LIGA process (Fig. 4a) [1]. This electrode array had 10 µm wall thickness and 300 µm height. It was used to fabricate gears (Fig. 4b) from 70 µm-thick tungsten carbide cobalt (WC/Co) super hard alloy plates. Using the electrode array provided throughput more than 100 times higher than that of serial µEDM using a single electrode.

Stents and Antenna Stents

The µEDM method has been used in the recent past to fabricate stents [19,20]. Stents are mechanical devices that are chronically implanted into arteries in order to physically expand and scaffold blood vessels that have been narrowed by plaque accumulation. Although they have found the greatest use in fighting coronary artery disease, stents are also used in blood vessels and ducts in other parts of the body. These include iliac, carotid, and renal arteries, biliary ducts and ureters. The vast majority of coronary stents are made by laser machining of stainless steel tubes, creating mesh-like walls that allow the tube to be expanded radially with a balloon that is inflated during the medical procedure, known as balloon angioplasty. A lithography-compatible method for fabricating these devices would be useful for the purpose of integrating sensors and sensing materials onto them. (It would also permit such 3D structures and assembly methods to be incorporated into the portfolio of micromachining techniques being used for other devices.) This type of ability to monitor pressure and flow can be useful because re-narrowing (restenosis) often occurs following a stenting procedure, and intraluminal wireless sensors for pressure or flow can be used in monitoring of the patency of the lumen.

A lithography-compatible approach can be used for machining stents and other tubular meshes without the need for bonded or welded seams [19]. The patterns, such as involute bands between a pair of side-beams, are cut into 50-µm thick stainless steel foil. In assembling the device, a deflated angioplasty balloon is threaded alternately above
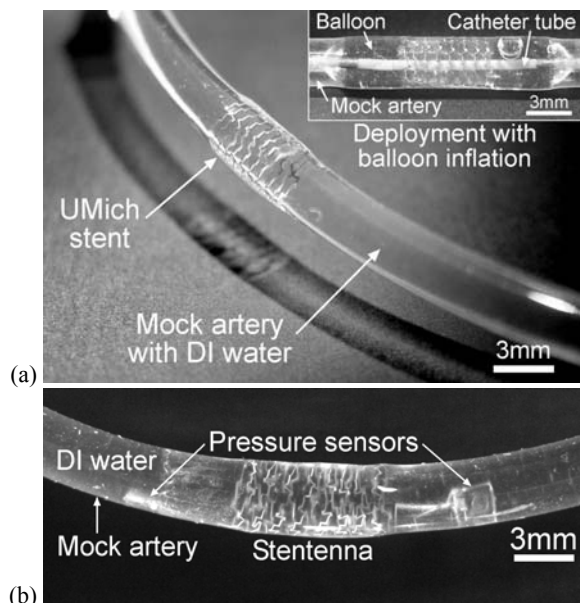
4

(a)

(b)

Fig. 5: (a) Stent fabricated from planar steel foil using µEDM and deployed within a mock artery using balloon angioplasty [19]. (b) The antenna stent coupled with two capacitive pressure sensors [20].

and below the bands, and then expanded by a normal angioplasty procedure. In [19], stents were expanded in two ways: inside mock arteries (Fig. 5a) and without external confinement (i.e. free-standing). Free-standing stents exhibited diameter variations of <±4 %, almost zero radial recoil after deflation of the balloon, and longitudinal shrinkage of <3 % upon expansion. Loading measurements demonstrated that the designs had radial strength similar to commercial stents.

In a further extension of this technology, a modified version of the stent was used as an inductive element in conjunction with a micromachined capacitive pressure sensor [20]. The inductive antenna stent (stentenna) was 20 mm in length and had 3.5-mm expanded diameter. It was coupled with capacitive elements to form resonant LC tanks that could be telemetrically queried (Fig. 5b). The resulting LC tanks were deployed inside silicone mock arteries using standard angioplasty balloons and used to wirelessly sense changes in pressure and flow. Using water as the test fluid, the resonant peaks shifted from about 208 MHz to 215 MHz as the flow was changed from 370 to 0 mL/min.

A variation of the fabrication approach for these stents uses strategically located narrowed beams or "necks" in the pattern, which serve as breakable links. As the links are broken during the balloon expansion process, the structure can be transformed from planar mesh to a helical shape. While breakable links are not necessarily suitable for stents, these features provide additional freedom in customizing the mechanical and electrical properties of these devices for other applications.

Related applications in the long term may include pressure sensors for abdominal aortic aneurysms, such as described by CardioMEMS, Inc. [21].
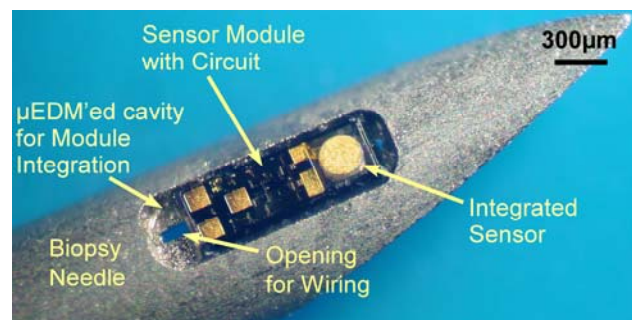

Fig. 6: Photograph of the tissue contrast sensing microsystem using piezoelectric sensors with integrated analog CMOS interface circuits [25].

Biopsy Tools

The ability of µEDM to pattern steel has also been useful in embedding micro-scale transducers into biopsy tools. The machining capability of µUSM on piezoceramics has been employed to form transducers for these applications. The work described in [22-25] was initially motivated by fine needle aspiration (FNA) of thyroid nodules. FNA biopsy is a common clinical procedure for harvesting cells from the thyroid, breast, etc. for subsequent cytological examination. It is typically performed with 20-27 gauge needles, with outer diameter <1 mm, and is challenging in itself due to the precision required in manually acquiring the desired sample from the small target volumes. Real-time ultrasound imaging provides only a partial solution despite the added complexity. For example, even with such imaging, at least 2-5% of thyroid FNAs are read as non-diagnostic because of improper sampling.

A passive sensor element was initially developed for detecting tissue contrast during FNA biopsy of thyroid nodules [22]. It used a micromachined PZT sensor in a thin disk form (50 µm thick and 200 µm in diameter) integrated directly into a 300 µm diameter cavity at the tip of a biopsy needle. The PZT sensor was made by batch µUSM and the needle cavity was formed by µEDM. The device is used to distinguish tissue planes in real time by measuring the electrical impedance spectra of the sensor with an impedance analyzer. The frequency and magnitude of an impedance resonance peak showed tissue-specific characteristics as the needle was inserted into testing tissue, and a proportional relationship between the frequency shift and sample acoustic impedance was found. A single wire located within the lumen supplied power to the sensor element; the wall of the needle served as the ground terminal. However, signal attenuation and stray capacitances caused by the needle tube and surrounding tissue can become substantial in certain tissue environments or at large insertion depths. The passive sensor cannot effectively differentiate tissue contrast when the needle penetration depth is greater than ≈15 mm, limiting its application in actual biopsy procedures, particularly for deep tissue.

The limitation in penetration depth can be alleviated by embedding active electronics in the needle (Fig. 6) [25]. An analog CMOS chip integrated with a piezoelectric sensor

5

can address the issues encountered with the passive device. It also eliminates the requirement of readout equipment such as the impedance analyzer, so that this technology can be potentially low-cost and widely accessible. A sensor element and CMOS circuit have been fabricated in-house at the University of Michigan, and integrated onto the tip of a 20-gauge biopsy needle. The sensor module with integrated interface circuit has a size of 950 µm (L) × 350 µm (W) × 220 µm (H). At this time, preliminary functional verification has validated the sensing system design. Ongoing efforts are directed at testing and performance evaluation of the microsystem, as well as tissue loading measurements in single and differential mode operation.

Although percutaneous biopsies are generally safe, potential risks include the deposition of viable tumor cells along the needle tract, and post biopsy hemorrhage. Cauterization of needle tracts is known to minimize these risks. A method for cauterization of the needle tract was reported in [23]. In this method, an array of 200 µm-diameter PZT disks was integrated at the tip of a 20-gauge biopsy needle. These PZT discs were used as heaters and generated a temperature rise of 33°C with an input power of <325 mW and drive voltage of <17 V_{RMS}. This heat is sufficient for tissue cauterization. The extent of cauterization in a test with porcine tissue was <1.25 mm beyond the perimeter of the needle, demonstrating the ability to control collateral damage to the surrounding tissue.

It is desirable to be able to detect the extent of tissue cauterization. An approach for monitoring the progress of the tissue ablation was reported using changes in the electromechanical impedance characteristics of the same PZT elements used for cauterization [24]. Cauterization of porcine tissue sample resulted in a decrease of 0.6 MHz in the resonance frequency and 900 ohms in the peak impedance magnitude, thereby indicating the extent of cauterization. This capability, along with the tissue-contrast detection for needle-tip-positioning guidance will provide, in the long term, a servo-controlled solution for biopsy and needle-tract cauterization of targeted tissue.

Single Crystal Quartz Resonators

The batch mode µUSM has been used for the fabrication of quartz crystal (QC) microstructures (Fig. 7) [15]. QC is widely used for sensing and timing applications. However, it is not amenable to most micromachining approaches. For example, wet etching of QC typically results in irregular sidewalls that depend on the crystalline planes. Multi-level AT-cut QC microstructures have been successfully fabricated by batch µUSM at a cutting rate >24 µm/min, which is substantially faster than available options for plasma-based etching. Arrays of disks, H-shaped and tuning fork structures are demonstrated with a cutting depth up to ≈105 µm on the 110 µm-thick QC substrate. Micromachined QC structures are also mounted on interconnection substrates and successful electrical tests have been performed to evaluate the resonance characteristics. A low-thermal-expansion glass ceramic,
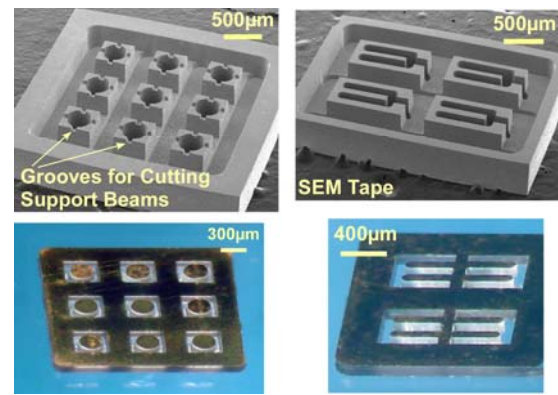

Fig. 7: (Upper two) Microtools made from stainless steel using µEDM; (Lower two) microstructures with multiple structural levels made from single-crystal quartz by batch mode µUSM [15].

Zerodur®, has also been micromachined at a cutting rate >18 µm/min.

In conclusion, it is evident that batch mode µEDM and batch mode µUSM can expand the bulk material options for lithographically machined microstructures. While additional work is needed to make these processes commercially robust, there are a number of devices to which these processes can be applied.

ACKNOWLEDGEMENTS

REFERENCES

[1] K. Takahata and Y. B. Gianchandani, "Batch mode micro-electro-discharge machining," *IEEE/ASME J. Micromechanical Systems*, vol. 11, no. 2, pp. 102-110, Apr. 2002

[2] T. Li and Y. B. Gianchandani, "A micromachining process for die-scale pattern transfer in ceramics and its application to bulk piezoelectric actuators," *IEEE/ASME J. Micromechanical System*, vol. 15, no. 3, pp. 605-612, Jun. 2006.

[3] K. Takahata and Y. B. Gianchandani, "Batch mode micro-EDM for high-density and high-throughput micromachining," in *Proc. IEEE Int. Conf. Micro Electro Mechanical Systems (MEMS 2001)*, Interlaken, Switzerland, Jan. 2001, pp. 72-75.

[4] D. Reynaerts, W. Meeusen, X. Song, H. Van Brussel, S. Reyntjens, D. De Bruyker, and R. Puers, "Integrating electro-discharge machining and photolithography: work in progress," *J. Micromechanics and Microengineering*, vol. 10, no. 2, pp. 189-195, Jun. 2000.

[5] K. Fischer, B. Chaudhuri, S. McNamara, H. Guckel, Y. Gianchandani, and D. Novotny, "A latching, bistable optical fiber switch combining LIGA technology with micromachined permanent magnets," in *Proc. 11th Int. Conf. Solid-State Sensors and Actuators (Transducers 2001)*, vol. 2, Munich, Germany, Jun. 2001, pp. 1340-3.

[6] T. Masaki, K. Kawata, T. Masuzawa, "Micro Electro-Discharge Machining and Its Applications," *Intl. Workshop*

on Micro Electro Mechanical Systems (MEMS '90), Napa Valley, California, pp. 21-26, February 1990

[7] T. Masuzawa, M. Fujino, K. Kobayashi, T. Suzuki, N. Kinoshita, "Wire Electro-Discharge Grinding for Micro-Machining," *Ann. CIRP*, v. 34, pp. 431-434, 1985

[8] K. Takahata, N. Shibaike, and H. Guckel, "A novel micro electro-discharge machining method using electrodes fabricated by the LIGA process," in *Proc. IEEE Int. Conf. Micro Electro Mechanical Systems (MEMS 1999)*, Orlando, FL, Jan. 1999, pp. 238-243.

[9] H. Guckel, "High-aspect-ratio micromachining via deep X-ray lithography," *Proc. IEEE*, vol. 86, no. 8, pp. 1586-93, Aug. 1998

[10] M.T. Richardson and Y.B. Gianchandani, "Achieving Precision in High Density Batch Mode Micro-Electro-Discharge Machining," *IOP Journal for Micromechanics and Microengineering*, vol. 18, no. 1, 015002 (12 pp.), January 2008

[11] M. Richardson, Y.B. Gianchandani, "Wireless monitoring of workpiece material transitions and debris accumulation in micro-electro-discharge machining," *IEEE/ASME J. Microelectromechanical Systems*, 19(1), pp. 48-54, February 2010

[12] T.B. Thoe, D.K. Aspinwall, and M.L.H. Wise, "Review on ultrasonic machining," *International J. Machine Tools & Manufacture*, vol. 38, no. 4, pp. 239-255, Apr. 1998

[13] X. Sun, T. Masuzawa, and M. Fujino, "Micro ultrasonic machining and its applications in MEMS," *Sensors and Actuators A (Physical)*, vol. A57, no. 2, pp. 159-64, Nov. 1996

[14] H. Choi, S. Lee, and B. Lee, "Micro-hole machining using ultrasonic vibration," *Key Engineering Materials*, vol. 238-239, pp. 29-34, 2003

[15] T. Li and Y. B. Gianchandani, "A high speed batch mode ultrasonic machining technology for multi-level quartz crystal microstructures," *IEEE International Conference on Micro Electro Mechanical Systems*, Hong Kong, pp. 398–401, 2010.

[16] K. Visvanathan, T. Li, and Y.B. Gianchandani, "3D-SOULE: A fabrication process for large scale integration and micromachining of spherical structures," *The 24th IEEE Int. Conf. Micro Electro Mechanical Syst. (MEMS 2011)*, Cancun, Mexico, Jan. 2011, pp. 45-48

[17] A. Matthews, and F.J. Rybak, "Comparison of hemispherical resonator gyros and optical gyros," *IEEE Aerospace and Electronic Systems Magazine*, 7, pp. 40-46, 1992.

[18] A.M. Shkel, C. Acar and C. Painter, "Two types of micromachined vibratory gyroscopes," *IEEE Sensors*, pp. 531-536, 2005.

[19] K. Takahata and Y.B. Gianchandani, "A Planar Approach for Manufacturing Cardiac Stents: Design, Fabrication and Mechanical Evaluation," *IEEE/ASME Journal of Microelectromechanical Systems*, 13(6), pp. 933-939, Dec. 2004

[20] K. Takahata and Y.B. Gianchandani, K.D. Wise, "Micromachined Antenna Stents and Cuffs for Monitoring Intraluminal Pressure and Flow," *IEEE/ASME J. Microelectromechanical Systems*, 15(5), pp. 1289-1298, October 2006

[21] M.A. Fonseca, M.G. Allen, J. Kroh, J. White, "Flexible wireless passive pressure sensors for biomedical applications," *Solid-State Sensors, Actuators and Microsystems Workshop (Hilton Head '06)*, S. Carolina, June '06, pp. 37-42

[22] T. Li, R. Y. Gianchandani, and Y. B. Gianchandani, "Micromachined bulk PZT tissue contrast sensor for fine needle aspiration biopsy," *Lab on a Chip*, vol. 7, no. 2, pp. 179-185, Feb. 2007.

[23] K. Visvanathan, Y.B. Gianchandani, "Biopsy Needle Tract Cauterization Using and Embedded Array of Piezoceramic Microheaters," *IEEE/ASME International Conference on Micro Electro Mechanical Systems (MEMS 10)*, Hong Kong, Jan. 2010, pp. 987-1000

[24] K. Visvanathan, T. Li, and Y.B. Gianchandani, "In situ monitoring of cauterization with a biopsy needle using impedance characteristics of embedded piezothermal elements," *14th Int. Conf. Miniaturized Syst. Chemistry and Life Sciences (µTAS 2010)*, Groningen, Netherlands, Oct. 2010, pp. 1478-80

[25] T. Li and Y.B. Gianchandani, "An active tissue-contrast sensing microsystem for biopsy needles: initial results," *The 24th IEEE Int. Conf. Micro Electro Mechanical Syst. (MEMS 2011)*, Cancun, Mexico, Jan. 2011, pp. 21-24

[26] F. Pacini and L.J. De Groot, "Thyroid Neoplasia," *The Thyroid and its Diseases*, 6th ed., W.B. Saunders Company, 1996, updated online at www.thyroidmanager.org, May 2004.